JOURNAL OF MATERIALS SCIENCE 37 (2002) 4247–4257

Failure paths at copper-base leadframe/epoxy molding compound interfaces

H. Y. LEE*
School of Mechanical and Aerospace Engineering, College of Engineering, Seoul National University, Seoul 151-744, Korea
E-mail: hlee@snu.ac.kr

G. S. PARK
Analytical Engineering Lab., Corporate TCS Center, Samsung Advanced Institute of Technology, P.O. Box 111, Suwon 440-600, Korea

Black-oxide and/or brown-oxide layers were formed on the surface of copper-base leadframe sheets in hot alkaline solutions, and then the oxide-coated leadframe sheets were molded with epoxy molding compound (EMC). The molded bodies were machined to form sandwiched-double-cantilever-beam (SDCB) specimens, and the adhesion strength between oxide-coated leadframes to EMC was measured in terms of critical energy-release rate (G_{IC}) using SDCB specimens. Results revealed that untreated leadframe and Cu_2O-coated leadframe showed almost no adhesion to EMC, however once a continuous CuO layer formed on the leadframe surface (brown oxide) or on the Cu_2O layer (black oxide), G_{IC} increased to around 80 J/m^2. A study of failure surfaces base on the scanning electron microscopy (SEM), glancing-angle X-ray diffractometry (XRD), Auger electron microscopy (AES), electron dispersive spectroscopy (EDS), and atomic force microscopy (AFM) analyses indicated that the failure path was closely related to the surface condition of leadframe prior to molding with EMC.

1. Introduction

Leadframes, together with the silicon chips, the gold wire and the epoxy molding compounds (EMCs), are one of the most important materials used in the plastic packages [1]. Copper-base alloys and Alloy 42 (Fe-42 wt% Ni) are the most widely used leadframe materials [2]. Recent trends of semiconductor packaging are rapidly heading toward higher integration and increased system speeds, which require a larger chip size as well as decreased package size. Along with these trends, the heat management with high integration and large chip size becomes an important issue [2].

Copper-base leadframes have been increasingly used as a major leadframe material in IC packaging due to their higher thermal and electrical conductivities, and lower cost relative to Alloy 42 (42 wt% Ni-Fe) leadframe [2]. However, they have a weak point from the viewpoint of package reliability [3–6]. Since copper-base leadframes bond to EMCs with lower adhesion strength than leadframes made of Alloy 42, the frequency of package delamination or cracking is higher than with an Alloy 42 leadframe. It has been reported that the low adhesion strength of copper-base leadframes to EMCs is caused by the low adhesion strength between the copper oxide layer and the copper in the leadframe [7]. Copper-base leadframe alloys are very susceptible to thermal oxidation when exposed to elevated temperatures in electronic packaging process, typically ranging from 150°C to 300°C for various time depending upon the type of materials used [1].

In the present work, attention was focused on the improvement of the adhesion strength between the copper-base leadframe and EMC to maintain good adhesion under harsh condition. The surface of a copper-base leadframe was modified by chemical oxidation treatments before molding it with the EMC and the adhesion strength of the leadframe to the EMC was then measured in terms of critical energy-release rate (G_{IC}) using sandwiched double-cantilever beam (SDCB) specimens. The fracture surfaces were then analyzed by various techniques to ascertain the failure path.

2. Experimental procedure

2.1. Formation of surface oxides

A commercial copper-base leadframe material (commercial name: EFTEC-64T, supplied by Amkor Technology Korea, Inc.) with the nominal composition of Cu-0.3Cr-0.25Sn-0.2Zn (by wt%) was provided in sheet form with a thickness of 0.15 mm. Organic impurities on the leadframe surface were removed by ultrasonic cleaning in acetone for 20 min and subsequently native oxides were removed by a pre-treatment solution (Activan #6, supplied by Han Yang Chemical

*Author to whom all correspondence should be addressed.

TABLE I The composition and temperature of the two treatment solutions

	Brown oxide [8]	Black oxide [9]
Composition	$NaClO_2$ (160 g/l) NaOH (10 g/l)	$NaClO_2$ (37.5 g/l) NaOH (50 g/l) $Na_3PO_4 \cdot 12H_2O$ (100 g/l)
Temperature	70°C	95°C

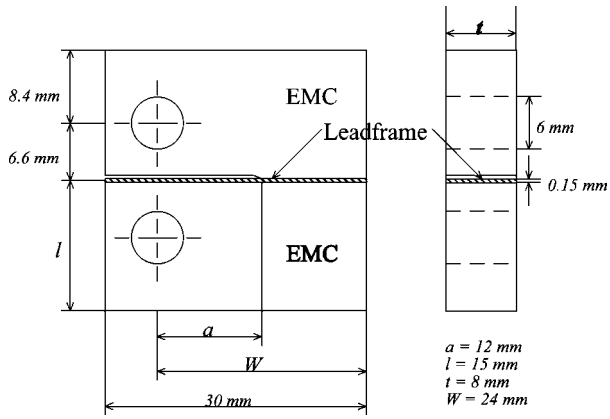

Figure 1 A schematic diagram of the sandwiched-double-cantilever-beam (SDCB) specimen.

Ind. Co. Korea). After the pre-treatment process, leadframe samples were immersed into hot alkaline solutions listed in Table I for less than 20 min to form brown-oxide [8] or black-oxide [9] layers on the leadframe surface. The surface oxides were analyzed by scanning electron microscopy (SEM) and glancing-angle X-ray diffractometry (XRD) with an incident angle of 2°, and the thickness of the oxide layers was measured by the galvanostatic reduction method [10].

2.2. Preparation of SDCB specimens and mechanical tests

After the formation of surface oxides, leadframe samples were compression-molded with EMC at a pressure of 6.5 MPa for 15 min at 175°C, and then machined into SDCB specimens as shown in Fig. 1. Pre-cracks were generated through pasting of correction tape on the leadframe surface, which is generally used for eliminating miswritten letters. The EMC used was DMC-20 developed as an encapsulation material for PLCC, VLSI, SOP, and FLAT packages by Dong Jin Chemical Co., Korea. After machining, post-mold curing treatment was carried out at 175°C for 4 h. Since an epoxy is a thermosetting polymer, post-mold curing treatment is needed to complete the polymerization reaction.

The SDCB specimens were employed to measure the adhesion strength in terms of interfacial fracture toughness under nearly mode-I loading conditions. Any homogeneous specimens for the fracture toughness tests can be converted into sandwiched specimens by inserting a sufficiently thin second material layer, and the solutions for energy-release rate, G, for homogeneous specimens are also applicable for sandwiched specimens [11]. According to the table in Ref. [11], the shift of phase angle due to the elastic mismatch, $\omega(\alpha,\beta)$, is about 3° for the EMC-leadframe system when the interlayer thickness (h) is taken as a characteristic length ($\hat{r}$).

The mechanical testing was conducted under a crosshead speed of 0.5 mm/min using tensile loading, and critical loads at which the onset of fracture process occurred were taken for the calculation of the interfacial fracture toughness [12]:

$$G_{\mathrm{IC}} = \frac{12P_C^2a^2}{t^2l^3\bar{E}}\left[1+\left(\frac{2l}{3a}\right)\right]^2 \qquad (1)$$

where G_{IC} and P_C are interfacial fracture toughness and critical load, respectively. $\bar{E}$ is a plane strain tensile-modulus defined as $E/(1-\nu^2)$ (ν: Poisson's ratio, E: Young's modulus), and a, t, and l are half crack-length, specimen thickness, and half specimen-height, respectively.

3. Results and discussion

3.1. Oxidation characteristics

3.1.1. Brown oxide

Scanning electron micrographs of oxidized leadframe surfaces treated in the brown-oxide forming solution are presented in Ref. [13] at various oxidation times. Fine acicular precipitates typically 0.1–0.3 μm in length covered the entire surface area after 1 or 2 min oxidation time. With further oxidation, the size and density of the precipitates increased slightly, and the precipitates remained almost the same as after 2 min of oxidation time. By subsequent X-ray and galvanostatic reduction analyses, the fine acicular oxide precipitates were shown to be cupric oxide (CuO) [13], and the thickness of the oxide layer was around 0.15 μm [13]. Once the CuO precipitates formed a continuous layer on the leadframe surface, there was no further nucleation of the CuO precipitates on the leadframe surface.

3.1.2. Black oxide

SEM micrographs of oxidized leadframe surfaces treated in the black-oxide forming solution are also presented in Ref. [13] at various oxidation times. There was no remarkable feature in the pre-cleaned surface, but smooth pebble-like precipitates formed after only a few seconds and coarsened to an average size of 0.2 μm after 0.5–1.0 min. The pebble-like precipitates with smooth facets were later identified to be cuprous oxide (Cu_2O). The average thickness of the Cu_2O layer increased up to about 0.2 μm within 1 min oxidation time. At an oxidation time of about 1 min, new acicular precipitates of 0.5–1.0 μm in length started to nucleate on top of the Cu_2O layer, and covered the whole leadframe surface after 2 min. The newly formed precipitates were afterwards confirmed to be cupric oxide (CuO). With further oxidation, the CuO layer thickened and became dense, but the size of the CuO precipitates remained nearly constant. The average thickness of the CuO layer increased parabolically with oxidation time, and reached 1.3 μm at 20 min oxidation time.

3.2. Fracture toughness

3.2.1. Brown oxide

The fracture toughness of leadframe/EMC interfaces was measured by employing SDCB specimens, and

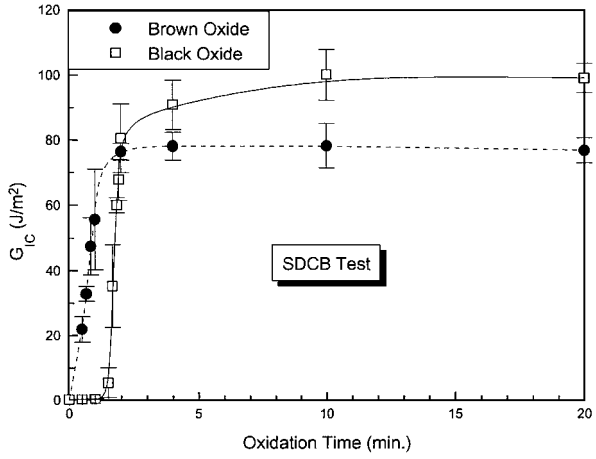

Figure 2 Nearly mode-I fracture toughness of the oxidized leadframe/EMC interfaces as a function of the oxidation time [13].

the results are shown in Fig. 2 [13]. For the leadframe/EMC system, the phase angle at the crack tip is about 3° [13]. Thus, the loading condition was close to a pure mode-I loading with a slight mode-II component (nearly mode-I loading condition).

The pre-cleaned only leadframe showed almost no adhesion to EMC ($G_{IC} \cong 0$ J/m^2), but as soon as the brown-oxide layer appeared on the leadframe surface, G_{IC} began to increase with oxidation time. It was observed that G_{IC} increased almost linearly with the oxidation time up to 1 minute and finally reached a saturation value of around 80 J/m^2 at 2 min. It seemed that the G_{IC} variation was remarkably close to the thickening kinetics of the brown-oxide layer, which indicates that the adhesion between the two materials occurs via mechanical interlocking: the acicular CuO needles penetrate into the epoxy resin in the EMC during the

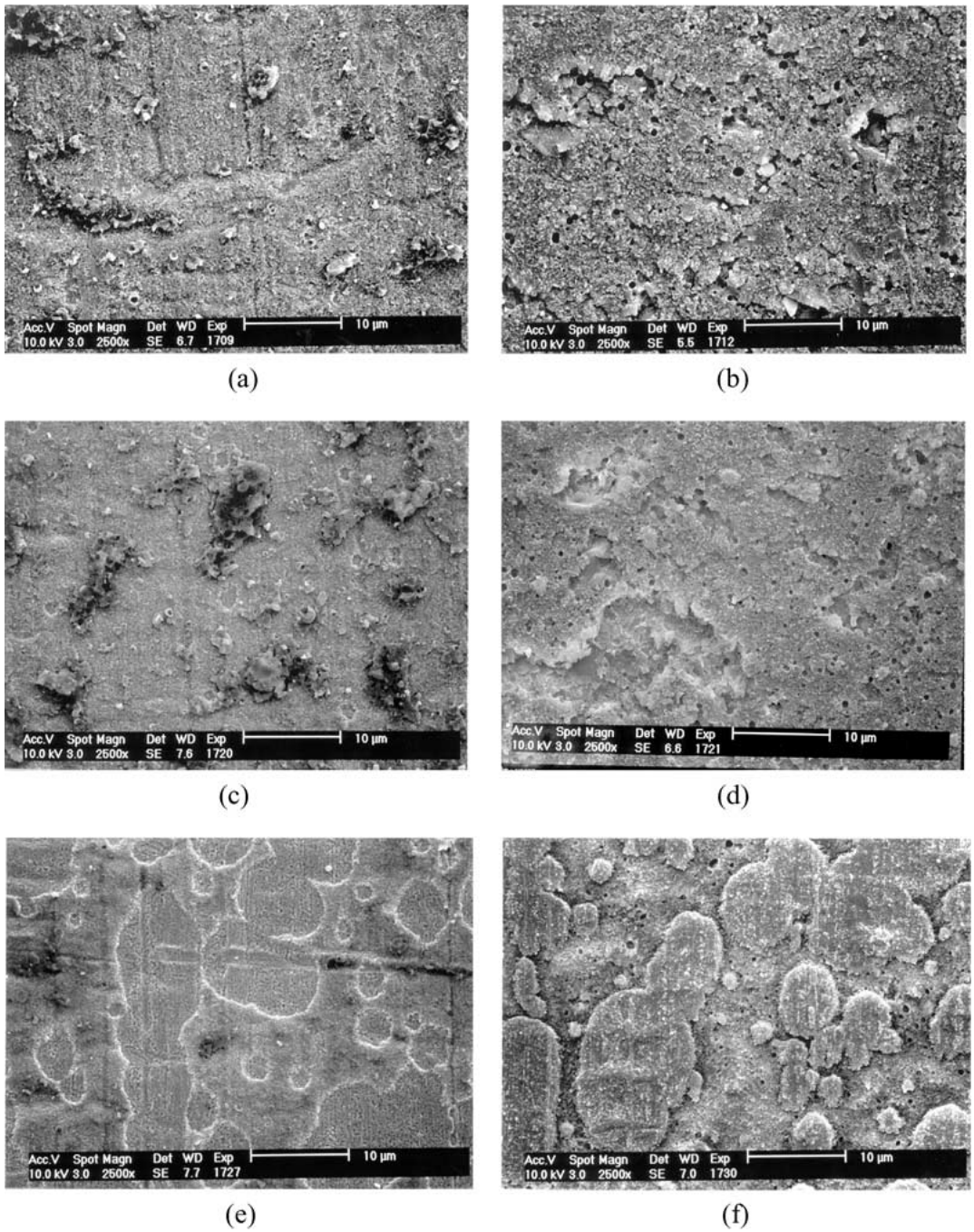

Figure 3 SEM micrographs of the separated brown-oxide-coated leadframe sides and EMC sides. (a), (c) and (e) are the leadframe sides with oxidation times of 30 sec, 1 min, and 2 min before molding with the EMC. (b), (d) and (f) are the EMC sides of the (a), (c) and (e), respectively.

molding process [13]. An implication of the present result is that the oxidation treatment for 2 min in a brown-oxide forming solution is good enough to provide a superior fracture toughness between the EMC and the leadframe.

3.2.2. Black oxide

The fracture toughness of leadframe/EMC interfaces was measured by employing SDCB specimens, and the results are shown in Fig. 2 [13]. The leadframe/EMC interface showed almost no adhesion ($G_{IC} \cong 0$ J/m^2) for 1 min. However, as soon as the acicular CuO precipitates formed on the Cu_2O layer, the G_{IC} began to increase and reached around 80 J/m^2 at 2 min. Further oxidation increased the G_{IC} gradually so that the G_{IC} reached a saturation value of 100 J/m^2 at around 10 min [13].

It was found that the presence of the pebble-like Cu_2O precipitates with smooth facets played no role in the adhesion, thereby provided no fracture resistance to the mode-I loading. However, the acicular CuO precipitates enhanced the fracture resistance. Therefore, it seems that the adhesion between the EMC and the CuO coated leadframe is attained through mechanical interlocking of the CuO needles into the epoxy resin.

3.3. Fracture surfaces analyses

It is well known that the adhesion strength is closely related to the fracture behavior of a joined body, and the fracture behavior of a joined body is governed by the material aspect of failure. Considerable efforts have been devoted towards fundamental understanding of the fracture behavior of joined bodies. To gain clues or pointers regarding the fracture behavior, a detailed examination of fracture surfaces is required, and a detailed examination of fracture surfaces should provide information about the failure path.

3.3.1. Brown oxide

SEM micrographs on the fracture surfaces are presented in Fig. 3. Comparing between micrographs taken

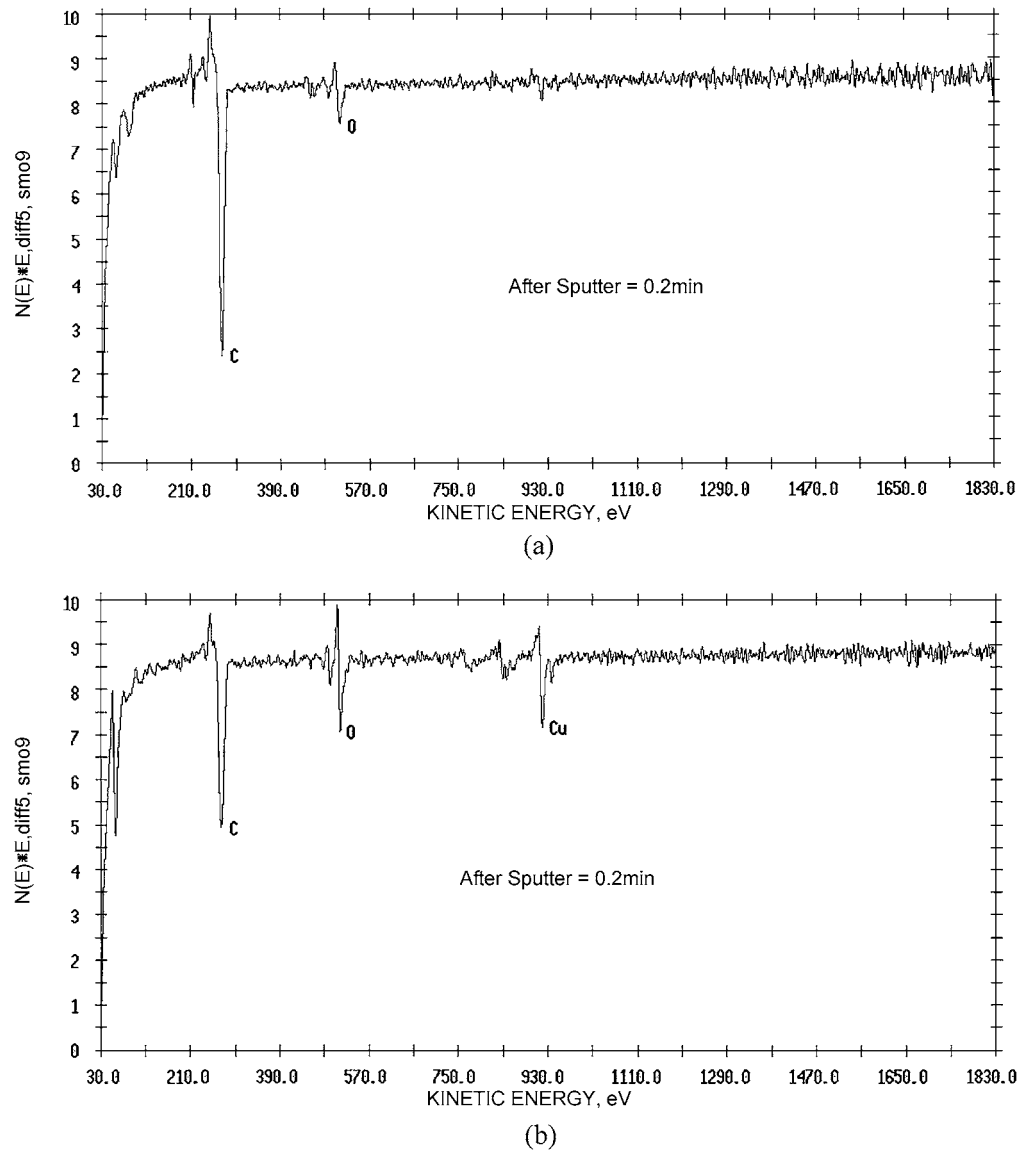

Figure 4 AES survey of (a) clod-like debris region and (b) non-debris region of the separated leadframe side of a brown-oxide coated leadframe/EMC joint, where the oxidation time of the leadfame before molding with EMC was 1 min.

from the separated leadframe and EMC sides, it can be stated that fractography was changed with the oxidation time: in the early stage of oxidation, non-dimple type (A-type) failure occurred, but when the oxidation time was more than 2 min, dimple type (B-type) failure took place.

For A-type specimens, clod-like debris with black color are seen on the separated leadframe sides (Fig. 3a and c), and their counterpart, separated EMC sides (Fig. 3b and d), were observed to be torn away severely. It is well known that brightness in SEM micrographs closely related to the emission rate of secondary electron: the brighter emission rate of secondary electron, the lighter images are acquired. The formulation for most EMCs consist of a complicated and often proprietary mixture of epoxy resin, hardener (or curing agent), catalyst(s), fillers, flame retardents, flexibilizers, coupling agents, mold release agents, and colorants. The EMC used in this experiment consists of epoxy resin of OCN (oxygen-carbon-nitrogen) type and some additives. The epoxy resin is known as nonconducting substance, the CuO is known as and p-type semiconducting substance [14]. The contrast on SEM micrographs may be due to the differences in electronic properties of the epoxy resin and the CuO. Normally the emission rate of secondary electron is higher for the semconducting materials than for the nonconducting materials [15, 16]. Considering leadframe and EMC were adhered together before mechanical tests and epoxy resin is relatively weak, the clod-like debris with black color on the separated leadframe sides are presumed to be EMC clumps.

To confirm the above inference, AES survey analyses was conducted on the two selected regions on the separated leadframe side of A-type specimen. The results are presented in Fig. 4. Since the carbon element could be introduced on the surface by contamination, it was necessary to confirm whether the carbon element came from surface contamination or not. To this effect, Ar-ion sputtering was carried out for 0.2 min as it is believed that the carbon element adsorbed from the surface contamination can be removed by Ar-ion sputtering. As expected previously, large amounts of carbon and oxygen elements exist on the surface of the clod-like debris after Ar-sputtering for 0.2 min (Fig. 4a). The presence of the carbon element on the separated

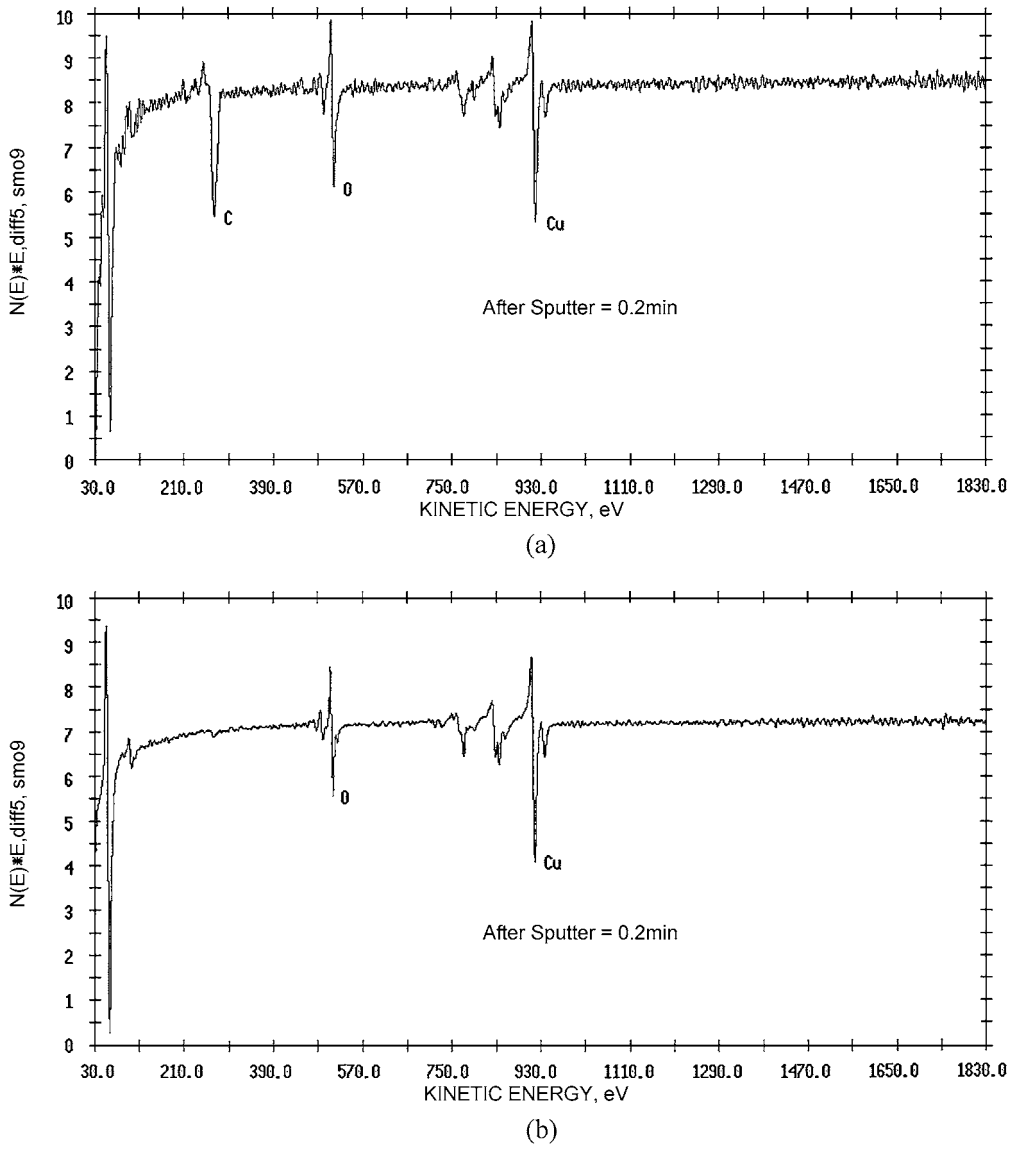

Figure 5 AES survey of (a) convex region and (b) concave region of the separated leadframe side of a brown-oxide coated leadframe/EMC joint, where the oxidation time of the leadfame before molding with EMC was 2 min.

leadframe side is probably due to epoxy resin in the EMC residue. Recalling that only the EMC has epoxy resin, it is supposed from the AES result that a cohesive failure in EMC predominantly occurred in the clod-like debris region.

On the other hand, three elements (carbon, oxygen and copper) were detected in the non-debris region (Fig. 4b). That might be attributable to the failure occurrence in the vicinity of the CuO/EMC interface. Since the CuO crystals have a needle shape, they interlock into the EMC so that the roughness of the CuO/EMC interface must be very high. Thus, in case of the occurrence of crack propagation along the CuO/EMC interface, a lot of carbon certainly comes to remain on the separated leadframe side.

For B-type specimens, cohesive failure was very likely to happen, because the dimple-shaped morphologies are seen from both SEM micrographs taken from the separated leadframe side (Fig. 3e) and its corresponding separated EMC side (Fig. 3f). To get more information about fracture surface, AES survey analyses were also carried out on the selected two regions of the separated leadframe side, convex region and concave region. The results are presented in Fig. 5. In case of the convex region, it is shown that the carbon element still exist in spite of Ar-ion sputtering for 0.2 min, and oxygen and copper elements also exist. The amount of carbon in the convex region was much more than that in the concave region. That indicates that carbon element in the convex region evidently originated from the EMC and oxygen and copper elements came from the CuO. With above results and the characteristic of the CuO/EMC interface, it can be said that fracture occurred in the vicinity of the CuO/EMC interface in the convex region. On the other hand, the concave region contains even less carbon element than the convex region does, and almost the same copper and oxygen elements. Taking it into consideration that the detection of oxygen and copper elements in the concave region and the constitution of the brown-oxide (CuO), it strikes that failure might occur in the CuO in case of the concave region.

To confirm the failure path mentioned previously, analyses on the copper distribution (Cu mapping) were conducted in the separated EMC side using EDS (electron dispersive spectroscopy). Note that the mapping information acquired by using EDS gives only qualitative information about specific element. The Cu mapping results are shown in Fig. 6. There is a lot of copper element in the convex region, however the opposite

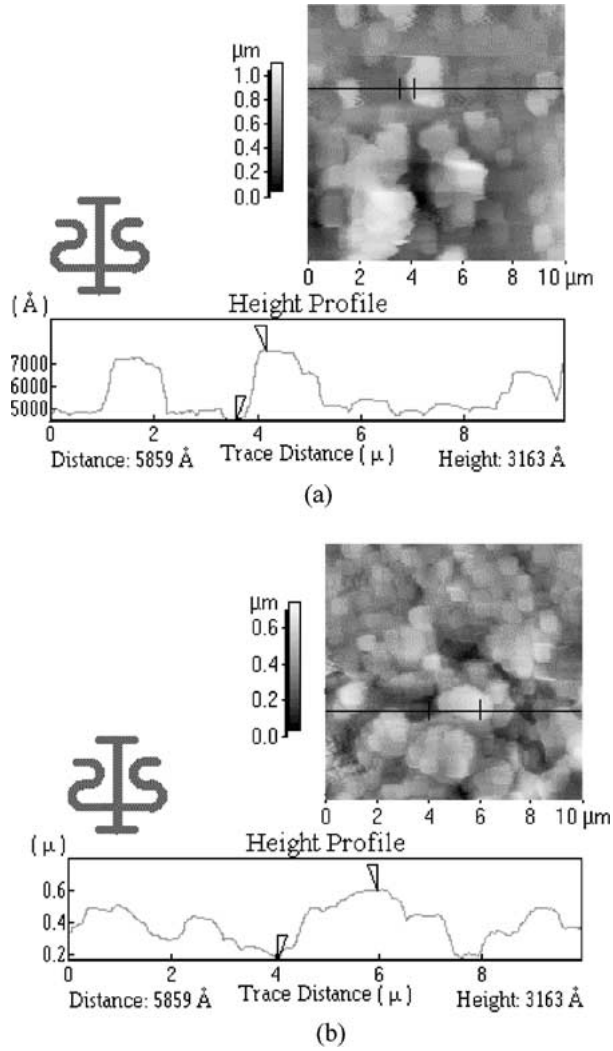

Figure 7 AFM images and line profiles of the separated (a) leadframe side and (b) EMC side of a brown-oxide coated leadframe/EMC joint, where the oxidation time of the leadfame before molding with EMC was 4 min.

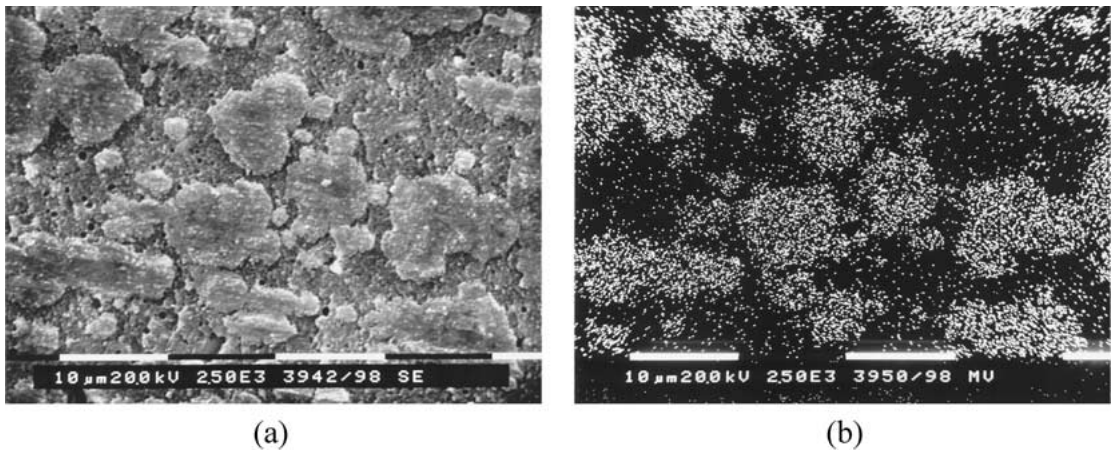

Figure 6 SEM micrograph and its corresponding copper-mapping image of the separated EMC side of a brown-oxide coated leadframe/EMC joint, where the oxidation time of the leadfame before molding with EMC was 4 min.

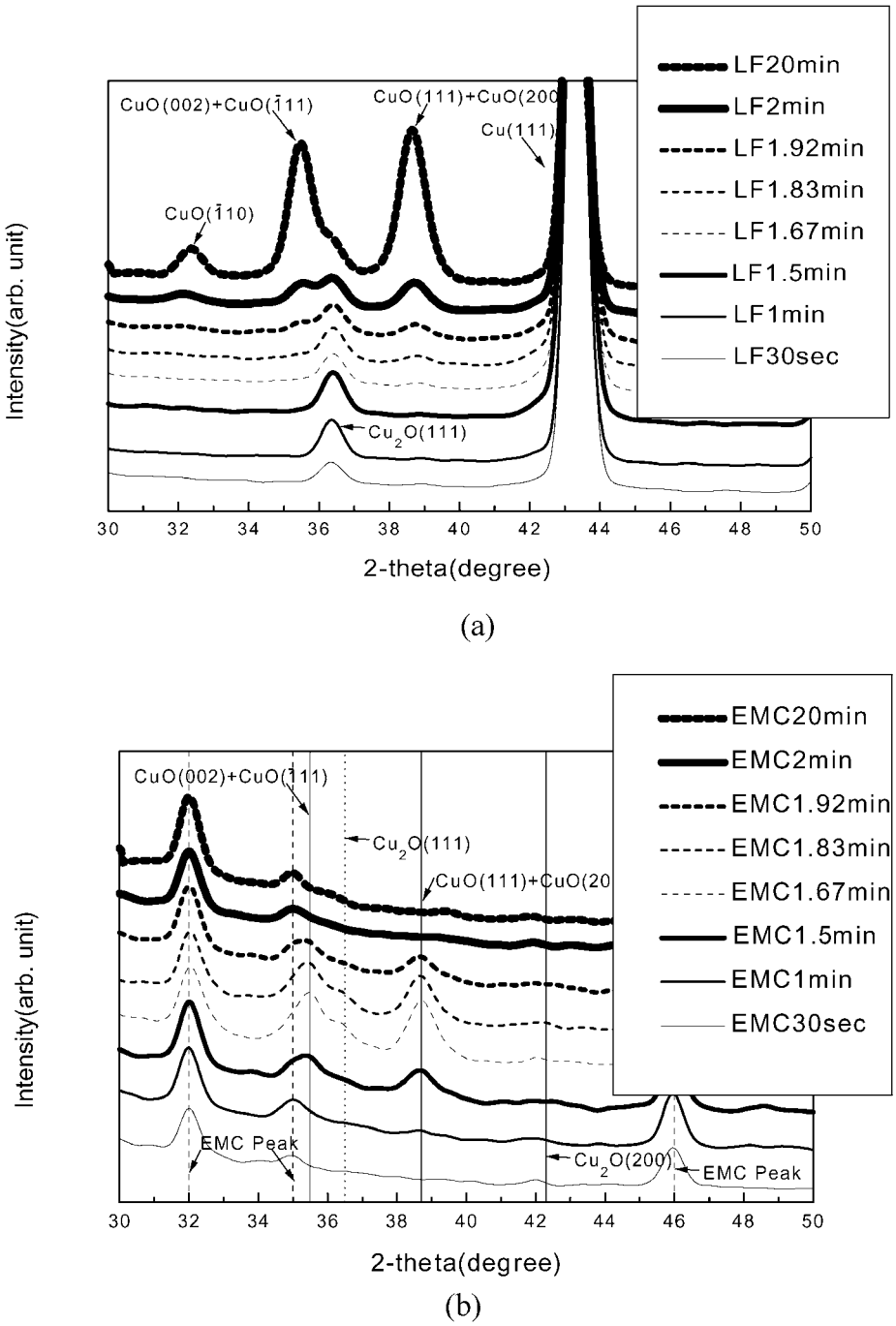

Figure 8 Glancing-angle X-ray diffraction patterns of the separated (a) leadframe side and (b) EMC side. The leadframes were treated in a black-oxide forming solution, and the times indicated in the plots mean oxidation times.

is true for the concave region. Recalling that EMC inherently does not contain copper element and the counter part of the convex region of the separated EMC side is the concave region of the separated leadframe side, EDS results support the previous inference that the cohesive failure occurred in case of the B-type specimens.

AFM analyses were conducted on the fracture surface to measure the differences in height between the convex region and the concave region. 10 μm $\times$ 10 μm area was selected, and roughness images and line profiles were acquired. The results were presented in Fig. 7. According to the line profile, the differences in height between the leadframe side and the EMC side were 316.1 nm and 440 nm, respectively. Considering the length of the CuO needles, these results are quite coincident with the previous AES results, the detection of carbon, oxygen and copper in the convex region.

3.3.2. Black oxide

After the fracture toughness testing, the separated leadframe and EMC sides were analyzed by glancing-angle XRD, and the results are presented in Fig. 8. As can be seen in Fig. 8a, the overall trend of separated leadframe side seems to be the same as that of as-oxidized leadframe shown in Ref. [13], but there were some differences. For example, after 2 min the height of the CuO(111) + CuO(200) peak was higher than that of the Cu_2O(111) peak for the as-oxidized leadframe, while the opposite was true for the leadframe side. On the other hand, X-ray analyses on the separated

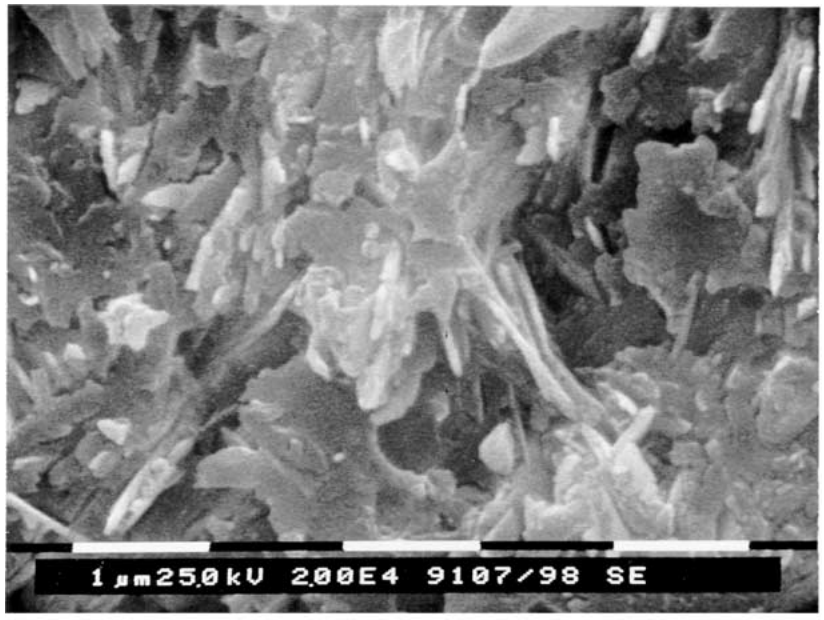

(a)

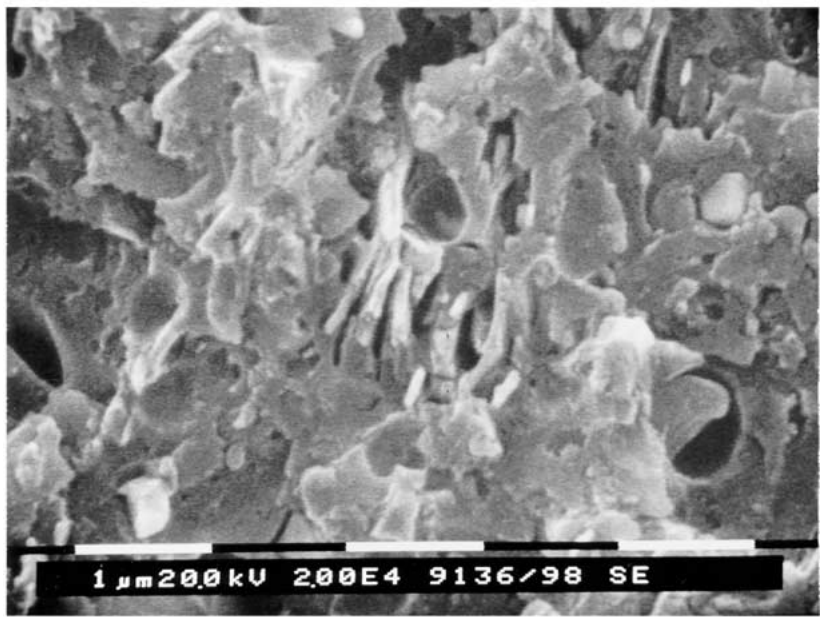

(b)

Figure 9 SEM micrographs of the separated (a) leadframe side and (b) EMC side of a brown-oxide coated leadframe/EMC joint, where the oxidation time of the leadfame before molding with EMC was 2 min.

EMC side revealed that there were only EMC peaks till 30 seconds and the CuO peak began to appear at 1 min and kept increasing till 1.83 min, but finally decreased. This might be ascribed to the detachment of the CuO whiskers from the leadframe surface. It can be confirmed from Fig. 9, which shows the traces of broken CuO whiskers on the separated leadframe side and embedded CuO whiskers on the separated EMC side.

AFM analyses were carried out on the as-oxidized leadframe and the separated leadframe and EMC surfaces. The results are shown in Fig. 10. In case of as-oxidized leadframe, since the Cu_2O has a smooth facets as shown in Ref. [13], the average roughness was relatively low when the Cu_2O was dominant on the leadframe surface. However, when the CuO was dominant on the leadframe surface, the average roughness was relatively high. This may be due to the acicular shape of the CuO as shown in Ref. [13]. Such a roughness change with the surface state of leadframe was well preserved in case of the separated leadframe. Comparing between the as-oxidized leadframes and the separated leadframes, one can readily find out that there is almost no difference in roughness. Such a good agreement may be ascribed to the similar nature of fracture surface.

The fracture surfaces were examined by using SEM, and results are shown in Fig. 11. The surface morphologies of separated leadframe which were oxidized for 30 seconds before molding are very similar to that of as-oxidized leadframe surface. For that reason, the surface roughness was relatively low and almost the same as compared to that of as-oxidized leadframe. Such smooth morphologies were well preserved till

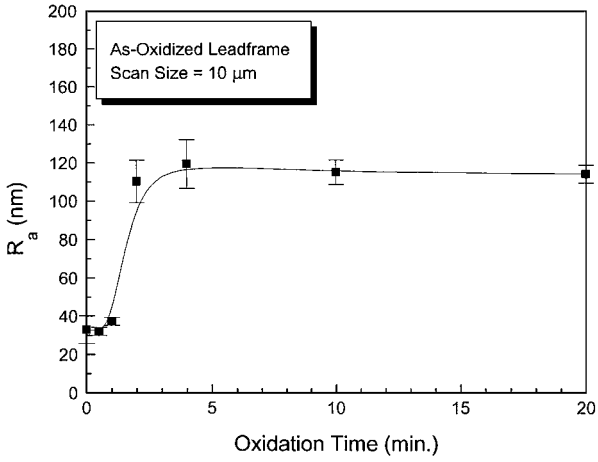

(a)

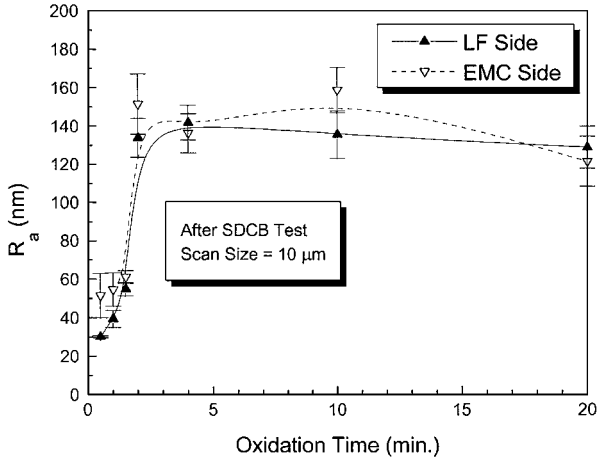

(b)

Figure 10 Variations of average roughness of the surface with oxidation time: (a) before molding, and (b) after SDCB test.

1.83 min. However, when the oxidation time was more than 2 min, the surface morphologies were abruptly changed so the morphologies were much rougher than to be seen. The measured roughness was relatively high and also almost the same as compared to that of as-oxidized leadframe. The reason why the average roughness of separated leadframes for oxidation time is more than 2 min is high may be ascribed to that the failure was occurred in the near the CuO/EMC interface.

3.4. Failure path

3.4.1. Brown oxide

Previous analyses on the fracture surface using SEM, AES, EDS and AFM showed that failure of the brown-coated leadframe/EMC interface ccurred in a mixed mode for both A-type and B-type specimens. When the oxidation time is below 2 min (A-type specimens), failure occurred in a nearly interfacial mode near by the CuO/EMC interface in the non-debris region of the separated leadframe side and in a cohesive mode in the inside EMC in the clod-like debris region. On the other side, when the oxidation time is more than 2 min (B-type specimens), nearly interfacial failure occurred in the vicinity of CuO/EMC interface and cohesive failure occurred in the inside of the CuO in the convex and the concave regions of the separated leadframe side, respectively. Schematic diagrams delineating the failure paths are shown in Fig. 12.

3.4.2. Black oxide

From the above good agreement among X-ray, AFM and SEM results, failure paths can be presumed to be the same as follows: when the oxidation time $t < 2$ min, fracture might occur in the EMC/Cu_2O interface ($t < 1$ min) or CuO/Cu_2O interface ($1 \leq t < 2$ min), which caused that the Cu_2O was left on the separated leadframe side so that the average roughness becomes nearly the same as that of as-oxidized leadframe. When the oxidation time $t \geq 2$ min, fracture might occur in the near the EMC/CuO interface. The failure paths can be schematically delineated with oxidation time in Fig. 13.

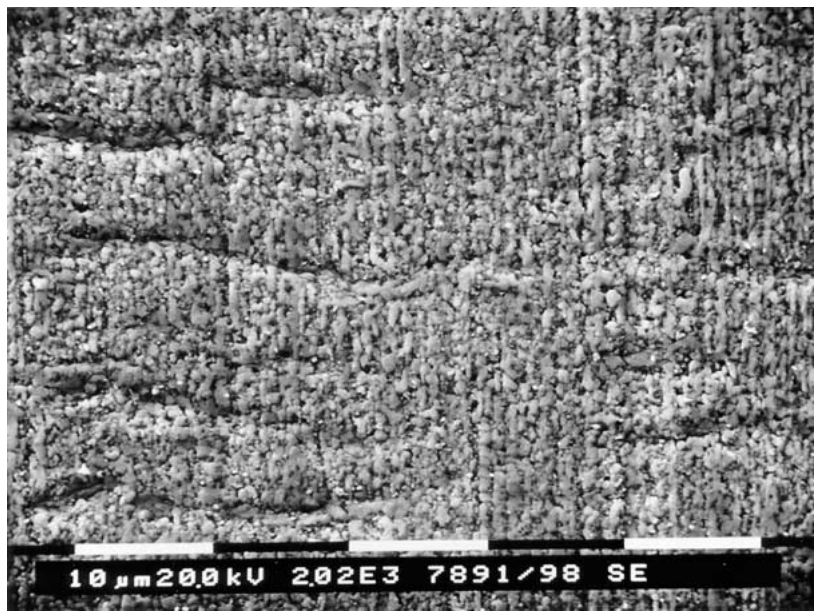

(a)

Figure 11 SEM micrographs of the separated black-oxide-coated leadframe sides. The oxidation times of leadframes before molding were (a) 30 seconds, (b) 1 min 50 seconds, (c) 2 min, and (d) 20 min. (*Continued.*)

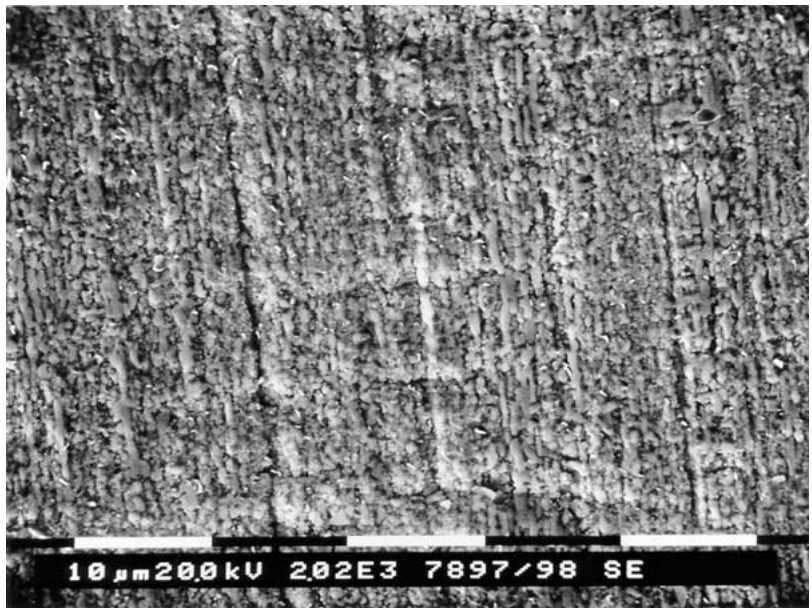

(b)

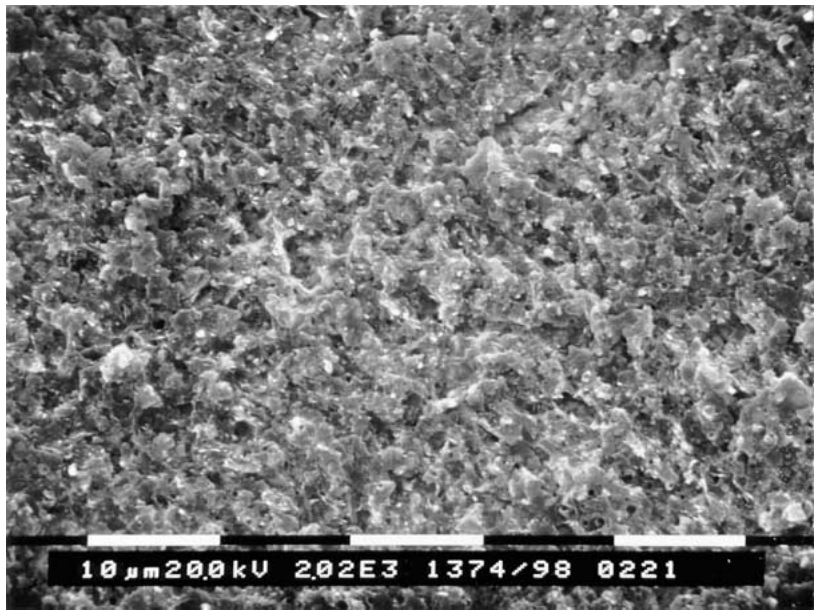

(c)

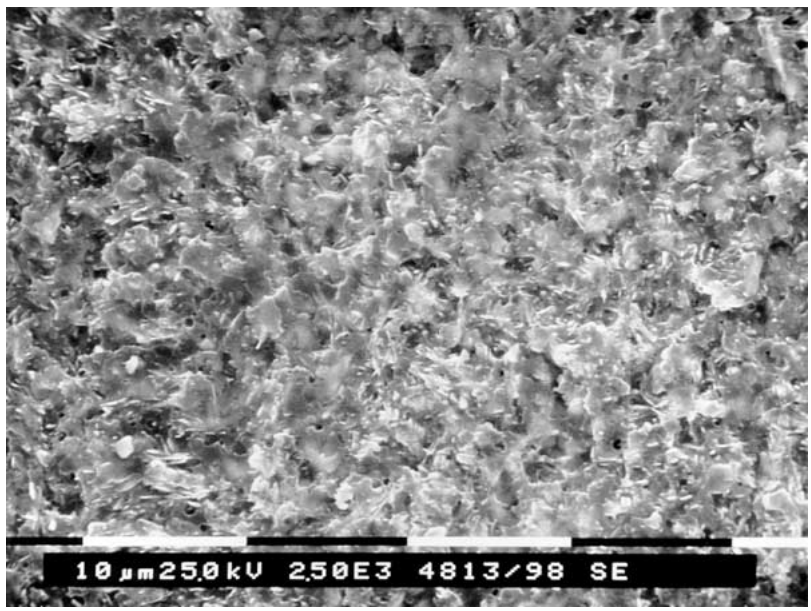

(d)

Figure 11 (*Continued*).

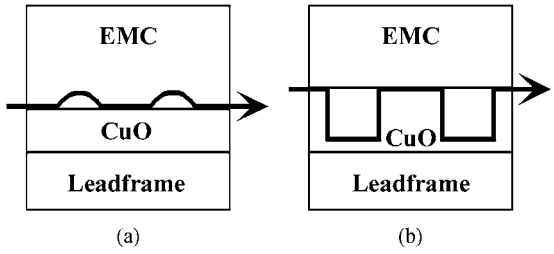

Figure 12 Schematic illustrations of failure path for the brown-oxide coated leadframe/EMC joints: (a) is for low oxidation time ($t < 2$ min), and (b) is for high oxidation time ($t \geq 2$ min).

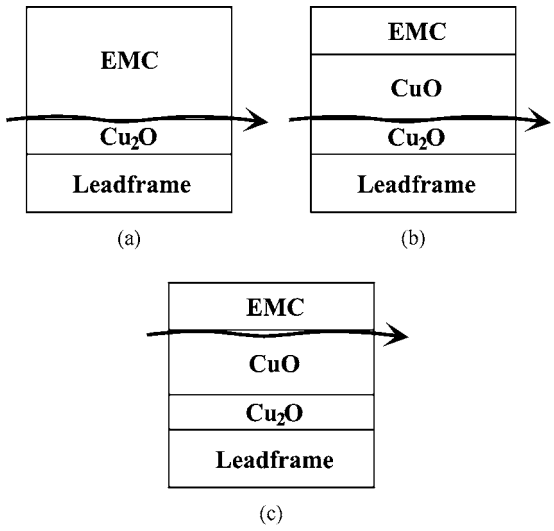

Figure 13 Schematic diagrams of failure path for the black-oxide coated leadframe/EMC joints: (a) is for the oxidation time, $t < 1$ min, (b) is for $1 \leq t < 2$ min, and (c) is for $t \geq 2$ min.

4. Conclusions

1. The fracture toughness of the brown-oxide-coated leadframe/EMC interface increased almost proportionally with the thickness of the CuO layer, and reached a saturation value around 80 J/m^2 at 2 min oxidation time.

2. In case of the brown-oxide-coated leadframe, fine acicular CuO precipitates on the leadframe surface increased the toughness of the leadframe/EMC interface by mechanical interlocking of the CuO needles into EMC.

3. After the fracture toughness tests of the brown-oxide-coated leadframe/EMC interface, systematic analyses on the fracture surfaces were carried out and the failure path was revealed: when the oxidation time is less than 2 min, failure path lies over near the CuO/EMC interface and inside the EMC, however, when the oxidation time is more than 2 min, failure path lies near the CuO/EMC interface and inside of the CuO.

4. The fracture toughness of the black-oxide-coated leadframe/EMC interface was nearly zero for the untreated interface, and remained so for the Cu_2O/EMC interface, too. However, once a continuous CuO layer formed on top of the Cu_2O layer, fracture toughness increased up to around 80 J/m^2 after 2 min oxidation time, and reached a saturation value around 100 J/m^2 after 10 min.

5. Acicular CuO precipitates contribute to the increase of adhesion strength, while the smooth-faceted Cu_2O played no role, which can be primarily ascribed to the acicular morphology of the CuO, causing mechanical interlocking with epoxy.

6. From the systematic analyses on the fracture surfaces after the fracture toughness tests of the black-oxide-coated leadframe/EMC interface, failure paths was disclosed: when the oxidation time, t, was below 1 min ($t < 1$ min), the leadframe surface was covered with Cu_2O, and the failure occurred near the Cu_2O/EMC interface. When the oxidation time was more than min but below 2 min ($1 \leq t < 2$ min), the leadframe surface was covered with a discontinuous CuO layer (mixture of the Cu_2O and the CuO), and the failure occurred in the vicinity of the CuO/Cu_2O interface. On the other hand, when the oxidation time was more than 2 min ($t \geq 2$ min), the leadframe surface was covered with a continuous CuO layer, and the failure occurred near the CuO/EMC interface.

7. The failure path was strongly dependent on the surface state of the leadframes before molding with EMC for both oxide treatments.

References

1. S. J. CHO and K. W. PAIK, *Scr. Mater.* **38** (1998) 1149.
2. S.-J. CHO, K.-W. PAIK and Y.-G. KIM, *IEEE Trans. CPMT*, B **20** (1997) 167.
3. G. L. ANG, L. C. GOH, K. W. HENG and S. K. LAHIRI, in Proc. 5th International Symposium on the Physical and Failure Analysis of Integrated Circuits (IPFA) (IEEE, Piscataway, NJ, 1995) p. 218.
4. T. SAITOH and M. TOYA, *IEEE Trans. CPMT*, B **20** (1997) 176.
5. S. YI, J. S. GOH and J. C. YANG, *ibid.* **20** (1997) 247.
6. S. YI and K. Y. SZE, *ASME Trans. J. Electronic Packaging* **120** (1998) 385.
7. S. KIM, *IEEE Trans. CHMT*, B **14** (1991) 809.
8. B. J. LOVE and P. F. PACKMAN, *J. Adhesion* **40** (1993) 139.
9. H. K. YUN, K. CHO, J. H. AN and C. E. PARK, *J. Mater. Sci.* **27** (1992) 5811.
10. J. R. G. EVANS and D. E. PACKHAM, *J. Adhesion* **9** (1978) 267.
11. Z. SUO and J. W. HUTCHINSON, *Mater. Sci. Eng.* A **107** (1989) 135.
12. T. S. OH, R. M. CANNON and R. O. RITCHIE, *J. Amer. Ceram. Soc.* **70** (1987) C352.
13. H. Y. LEE and J. YU, *Mater. Sci. Eng.* A **277** (2000) 154.
14. D. A. JONES, "Principles and Prevention of Corrosion" (Maxwell Macmillan, 1992) p. 411.
15. M. CAILLER and J.-P. GANACHAUD, in "Scanning Microsc. Suppl.," 4th ed., edited by J. Schou, P. Kruit, and D. E. Newbury, p. 57.
16. *Idem.*, "Scanning Microsc. Suppl.," 4th ed. edited by J. Schou, P. Kruit and D. E. Newbury, p. 81.

Received 6 July 2000
and accepted 23 April 2002